CHAPTER

V

D.C.ELECTRICAL CONDUCTIVITY AND THERMOELECTRIC POWER

5.1 Introduction

The importance of an understanding of conductive processes cannot be overestimated. Besides the obvious application to thermistors and barrier layer capacitors, the ability to control conductivity and usually to keep it very low, is highly important to the piezoelectric uses of ceramics. Compositions which are too conductive are difficult to pole, tend to overheat in high power applications, and generally have undesirably high dielectric loss which limits its efficiency.

Electrical conductivity is one of the essential characteristics of a substance and the elucidation of the conductivity is of primary importance. In particular, the electrical conductivity of ferroelectrics with simplest perovskite structure is not well understood. It is found that the point defects are responsible for many electrical properties of ABO3 (A=Pb, Ba, Sr; B= Ti) oxides belonging to perovskite family. The first step in the understanding of electrical transport in any solid is to know whether conductivity is ionic or electronic or mixed (Partially ionic and electronic). There are several ways of determining the nature of conductivity. The simplest way is to measure the d.c.conductivity as a function of time using electrodes which block ionic conduction. In the case of pure ionic conduction, d.c. conductivity decreases with time and tends to become zero after sufficiently long time, where as for a pure electronic conductor it is essentilally independent of time for mixed conduction it decreases with time but tends to stabilize at some finite constant value, which is the electronic contribution.

As far as ionic conductivity is concerned, interstential conduction seems difficult. Owing to very compact structure of a perovskite. Therefore creation of vacancies in the ceramic because of incomplete solid-state reaction or doping, appears to be the possible source for ionic or electronic conduction. It has been observed that the perovskite structure tolerates a substantial amount of vacancies,(96). Therefore, variation of conductivity with substitution is to be discussed in the light of possible mode of vacancy formation.

The seebeck co-efficient measurements on these systems indicate, whether the conduction is due to holes or electrons. A position vacancies in ABO_3 system attract electrons to complete the electronic shell of the surrounding oxygen, they act as an acceptor causing the presence of holes in the lattice according to the relation

$$VA \longrightarrow \overline{V}\overline{A} + 2h \qquad ----(5.1)$$

Where V represents a vacancy. Similar effects are produced because of substitution also, A positive ion replacing a higher valance cation acts as an acceptor that is K^{+1} for Ba^{+2}. In contrast a positive ion replacing another of lower valency acts as a donor e.g. Sb^{+5} for Ti^{+4}. Resistivity of single crystal $BaTiO_3$ is very large, of the order of 10^{12} Ω cm and shows a intrinsic conductivity both above and below the transition temperature. In case of ceramics the pores and imperfections create the donor and acceptor sites reducing the order of resistance.

Semiconducting n-type polycrystalline barium titanate can be prepared by partially substituting Ba^{+2} by a small amount of

trivalent cations such as rare earth elements, or Ti^{+4} by pentavalent cations such as Nb^{5+} Sb^{+5}. The defects are compensated by free electrons in the conduction band. The doped $BaTiO_3$, sintered in air, exhibits a very high relative permittivity,compare to the relative permittivity of undoped $BaTiO_3$, and an anomalous sharp increase in resistivity known as a PTCR effect above the ferroelectric paraelectric transition temperature.

Various models have been proposed to interpret the relative permittivity and PTCR behavior in doped $BaTiO_3$(97,98,99,100). The most satisfactory model that explains the PTCR is the Heywang model(97,99). The effects are attributed to the existence of potential barriers at the grain boundary regions, thought to be caused by acceptor type surface states. This model attributes the shape of the PTCR above the Curie Point to a rapid decrease in relative permittivity, which leds to a sharp rise in the height of the grain boundary potential barrier. Jonker (98) has modified this model by proposing that the spontaneous polarization of ferroelectric phase at the end of alternate domains below the Curie Temperature could effectively compensate the surface state charge, eliminating the potential barrier height, and hence led to the observed low resistivity of this material.

Extensive investigations are carried out by many workers to study the effects of sintering conditions (101), porosity(102,103) and defect structure on PTCR and relative permittivity of doped $BaTiO_3$ (104,105). Further the electrical properties of semiconducting ceramics, have been found to be very sensitive to the nature of the electrode materials(106,107).

The $BaTiO_3$ in the dense ceramic form or the compositions where the substitutions are off compensated off-Valency, the electron transport properties is the intermediate case of the two extremes viz. single crystal $BaTiO_3$ and n-type doped, porous or with structurally imperfect $BaTiO_3$. The n-type doped ceramic shows a drastic increase in the conductivity of the material as compared to that of single crystal $BaTiO_3$. As discussed above PTCR effect is observed in a few systems(108). The effects those are observed for acceptor doping are different from those observed for donor doping. The doping single crystals with 0.2 % Fe^{+3} increased the resistivity from 10^{12} to 10^{13} ohm cm, but further additions caused the Resistivity to decrease slowly (109,110). The situation regarding compensated off-valency substitution thus become a little complicated to be analyzed and the Resistivity is observed non Arrehenius. In the recent years the thirst is shifted from the measurement of D.C. resistivity to the measurement of complex impedance plots.(107,111). The complex impedance plots explained the apparent non Arrhenius behavior of the resistivity. From the complx impedance curve it is observed that in the vicinity of Curie temperature the complex impedance curves could be resolved as two semicircles. The semicircle corresponding to the higher frequencies represents the impedance of the bulk of grain, while the one at lower frequencies represent the impedance of the grain boundary . Using the an appropriate equivalent circuit models as in Fig. 4.7, the values of resistivity for the bulk of grain and grain boundaries are separated. Each one of these follow an Arrhenius behavior (64). Using analysis of complex impedance curves the resistivity of ceramic $BaTiO_3$ has been resolved to behave in Arrhenius fashion

by R.Flores et al (47). Similar analysis is also performed for $LiTaO_3$(95).

5.2 Theoretical Models for the Electron Transport Properties:

5.2.1 The Potential Barrier Effect on Resistivity:

According to the model of Heywang explaining the PTCR effect(97,99), the increase of resistivity above the curie temperature is caused by potential barriers at the grain boundary. The relation between the resistivity $\varsigma(T)$ and the height of the potential barrier $e\phi(T)$ at temperature T is given by (99)

$$\varsigma(T) = \varsigma_0 \exp [\, e\phi(T)/ KT] \quad \text{------} \quad (5.2)$$

and

$$e\phi(T) = \frac{e^2 Nd}{2\, CL(T)\, Co} x2 \quad \text{-------} \quad (5.3)$$

Where e is the charge of electron $\epsilon_L(T)$ is the relative permittivity at the grain boundary layer at temperature T. ς_o is a constant, k is the Boltzmann constant and x is the width of the grain boundary which can be given as

$$x = \frac{ns(T)}{2Nd} \quad \text{-----} \quad (5.4)$$

Where ns(T) is temperature dependence of the density of occupied acceptor states. ns(T) is given by the equation(99)

$$ns(T) = Ns \left[\, 1 + \exp\left(\frac{E_F + e\phi - Es}{KT} \right) \right]^{-1} \quad -(5.5)$$

Where Ns is the total acceptor density.Es is the acceptor energy and E_F the Fermi energy.

$$E_F = KT \ln (No/Nd)$$

$$No = (1.56 * 10^{28}) m^{-7} \quad \text{---------- (5.6)}$$

Where No is the number of Ti ions per m^3 (the effective density of states) (98). Nd can be calculated from the relation (105).

$$Nd = 1/e\mu \rho_g$$

Where μ is the electron mobility and equal to $(5 * 10^{-5})$ m^2V^{-1} S^{-1} (105): ρ_g is the bulk resistivity which can be calculated from the resistance of the bulk (2 ohm) and the sample dimensions.

In order to describe the PTCR effect by using the Heywang model and account for the measured (apparent) resistivity $\rho(T)$ and measured relative permittivity $\epsilon m(T)$ of the sample under investigation, a small modifications of the theory has been made by Kuwabara et al (103) and Al-Allack et al (112)> .The relation between $\epsilon m(T)$ and $\epsilon L(T)$ is written as

$$\epsilon m(T) = \epsilon L.1(T)d/2x \quad \text{--------(5.7)}$$

Where d is the average grain size(about 10μm). Substituting equation 5.7 and 5.4 in to equation 5.3 one can get

$$e\phi(T) = e^2 ns(T) d/ 8\epsilon o\epsilon m(T) \quad \text{----(5.8)}$$

Equation 5.8 show that $e\phi(T)$ is inversely dependent on the measured $\epsilon m(T)$, assuming that Nd and x are constants and ns(T) is

also constant in the vicinity of Tc. The PTCR effect may be described by substitution of equation 5.8 in to equation 5.2 to get the equation

$$\varsigma(T) = \varsigma_o \exp\left(G/ \epsilon_m(T)\, T\right) \text{----(5.9)}$$

or

$$\ln[\varsigma(T)] = \ln \varsigma_o + \frac{G}{\epsilon_m(T)\, T} \text{-----(5.10)}$$

Where $G = e^2 n_s(T) d/8\epsilon_o$ ----- (5.11)

If $n_s(T)$ was not constant then using the equation 5.5 the density of occupied acceptor states $n_s(T)$ could be calculated. Further from equation 5.2, 5.9 and 5.10, $e\phi(T)$ can be written as

$$e\phi(T) = \frac{KG}{e\, \epsilon_m(T)} \text{------(5.12)}$$

Attempt could be made to fit the experimental $\varsigma(T)$ with the theoretical model by solving numerically equations 5.5, 5.6, 5.12 i.e. equation of resistivity

$$\varsigma(T) = \varsigma_o \exp\left[\frac{(e^2\, n\, T\,)d}{8\, K\, T\epsilon_o\, \epsilon_m\,(T)}\right] \text{------(5.13)}$$

The theoretical depedance of $\epsilon_m(T)$ on temperature has been given by the Curie-Weiss law. Different values of acceptor or energies Es and Acceptor- state densities Ns have been used to get a better fit between theoretical and experimental values of D.C. and A.C. resistivity with temperature in the region of PTCR. Though this theory accounts for the relation between ϵ_m and , it is insufficient to account for complete non Arrhenius

behavior observed in compensated off- valency substituted $BaTiO_3$. Further ϵr versus T exhibits a diffused transition in these cases.

5.2.2. A Qualitative Model for Electron Transport in Ceramic $BaTiO_3$

As it has been discussed in previous section that the overall behavior of $\rho(T)$ or $\sigma(T)$ is non Arrhenius for the ceramic $BaTiO_3$. So also is the case of compensated off-vacancy substituted $BaTiO_3$. As discussed in the section 5.1, the attempts in last a few years are towards measurement of z'' versus z' as a function of frequency and separation of contributions Cb,Rb,Cd, and Rd. Fig. 4.7.

In our opinion this procedure does not throw any light on the physical mechanism explicitly for occurrence of temperature depedance of these parameters .Therefore one needs to think of some model which can account for the diffused phase transition, electrical conductivity, thermopower and if possible increase of value of ϵr, at fixed frequency, in the paraelectric region. Here we wish to propose a model to account for electrical conduction. At present we are just proposing the model and wish to account qualitatively the observed electrical conductivity σ and thermopower(Q) for SbMn and SbCo compositions. This model has a few similarities with the model of potential barrier effect discussed in section 5.2.1.

Fig 5.1 shows the band model which is proposed to take care of both the PTCR and/or non Arrhenius behavior observed.

The band model of Fig. 5.1 shows the conduction band the

valance band, the donor and acceptor energy levels, energy midpoint of the band gap, and the Fermi energy E_F as a function of temperature variation. The various other parameters are also required to be considered. These parameters include the density of donor impurities Nd, density of acceptor impurities Na, the values of Edp, Edf, Eap and Eaf, For a given situation we may consider a few approximations and make the model simpler. For example in the case of donor doped $BaTiO_3$ we may assume Nd>>Na. Nevertheless a few general conditions are to be observed always. The conditions are

1) During the region of phase transition the Edp and Edf, Eap and Eaf join smoothly. The curvature of Ed and Ea lines may have a numeric correlation to the variation of Cr as a function of temperature in this region.

2) Ed > Ea this condition is required to explain the increased hole conductivity in the paramagnetic region of doped and undoped $BaTiO_3$. Using the basic theory of extrinsic semiconductor and the proposed band model we can write the following equations for number of electrons in the conduction band n(T), number of holes in the valance band P(T), conductivity and the thermoelectric power as given below.

$$n(T) = \frac{Nd - Na}{2\,Na} Nc \exp\left[-(Ec-Ed)/KT\right]$$

Where Nc is the density of states in the conduction band.

P(T) this value is to calculated using the mass action law, thus

$$Ni^2 \quad P(T) = \frac{\quad}{\quad} \quad n(T)$$

$$\sigma = e[\, n(T)\mu_n + P(T)\mu_p]$$

$$Q = -\frac{K}{q}\left|\frac{[5/2 - S + \ln(Nc/n)]\, n\mu_n - [5/2 - S + \ln Nv/p]p\mu_p}{n\mu_n + p\mu_p}\right| \qquad \text{----------(5.14)}$$

Where S is a constant determined from the relaxation time behavior.

While applying this model for numeric calculation of σ or Q the band gap Ec - Ev could be determined from the experimental behavior of ln σ as function of (1/T).

The remaining parameters are to be calculated under certain assumptions from the experimental fit and the concentrations of donors and acceptors added into the $BaTiO_3$ matrix.

The thermoelectric power (Q) could be calculated using the well known Mott relation as an alternative to the equation 5.14. This form of the Q is given as

$$S(T) = \frac{\pi^2 K_B^2 T}{3|e|}\left|\frac{d\ln\sigma}{dE}\right|_{E_F} = \frac{-\frac{2}{\pi} K_B^2 T \xi_s}{3|e|E_F}$$

In this case we may need to determine the function ξ_s from the experimental values of ln (σ).

5.3 Result and Discussion:

5.3.1 Log σ behavior of SbMn system.

The Fig. 5.2 to 5.6 shows the Logσ as a Function of (1/T), for $Ba\ Ti_{(1-x)}\ Sb_{x/2}Mn_{x/2}\ O_3$ system with x = 0.025, 0.05, 0.1, 0.2, 0.4. respectively. Theoverall behavior of log σ is non Arrhenius and the behavior show a break in slope at two different temperatures. The temperature at which break in slope is detected are given in table 5.1. It is observed from the table that the break in slope occurs at a higher temperature for x=0.025 and x=0.4 other wise the break in slope is very near to the room

temperature. The temperature of break in slope should be correlated to the behavior of ϵ_r as (T). The behavior of ϵ_r as(T) represents the diffused phase transition and a single temperature cannot be defined as the curie temperature. The variation of ϵ_r as (T) shows a very broad transition for x = 0.025.The ϵ_r reduces from its maximum value in the temperature range of room temperature to $\approx 420^{\circ}K$. The temperature $375^{\circ}K$ of break in slope lies in this region. In case of ferroelectrics with diffused phase transition it is observed that the parameters like refractive index (66), Specific heat (89), Thermal expansion (91) etc deviate from their normal behavior for temperatures of afew tens of degrees from Tc. The break in slope occurring at a different temperature than the Tc could be attributed to this effect. For x=0.4, the reasoning given above doesn't follow strictly. In this case we may have another break in slope below room temperature, which is not determined in the present investigations.

As far as the room temperature values of conductivity is concerned Table 5.1, it is observed that for x=0.025 the conductivity is maximum and the same sample shows a mild PTCR . Nevertheless diffused PTCRs are observed for almost all the samples. The increase conductivity for x= 0.025 has a correlation with change in parameter 'a' observed from the structural investigations.

The log 6 versus 1/T shows another break in slope at higher temperatures. The ϵ_r is also observed to pass through a peak. The temperatures of the second peak are rather insensitive to the concentration x. Similar insensitivity is observed in case of the break in slope in the log 6 behavior.

5.3.2: Log 6 behavior of SbCo System

The Fig. 5.7 to 5.11 show the log 6 as a function of (1/T), for Ba $Ti_{(1-x)}$ $Sb_{x/2}Co_{x/2}$ O_3 system with x = 0.025, 0.05, 0.1, 0.2, and 0.4 respectively. The over all behavior of log 6 is non Arrhenius in this case also . Two breaks in slope are detected for all the concentrations of SbCo. The temperature at which break in slope occurs and Er versus T behavior have similar correlation as in case of SbMn system, We shall not repeat the quantitative logic presented for SbMn system, but the explanation would be more or less similar in this case also.

Despite of this similarity the room temperature conductivity of SbCo system decreases slowly as the concentration is increased. This could be attributed to the oxygen vacancies probably in SbCo system(64), At higher and higher concentration of SbCo the Co^{+2} ions may induce additional acceptor sites . We expect the thermopower will reflect this increase in acceptor states.

5.3.3 Thermoelectric Power of SbMn And SbCo systems:

As far as literature Survey is concerned only a few references are available on the measurement of thermopower Q of the $BaTiO_3$ and related compositions. In our opinion the reason could be the difficulties in setting up of the experiment for the measurement of Q, may reveal the information which is aother wise available from the conductivity meaasurements. But the Q is proportional to $\left.\frac{d\ln\varsigma}{dE}\right|_{E=E_F}$

and may provide a very critical information of the electron transport in the phase transition region. The region where the

Fig 5.1 The Schematic of Band Model.

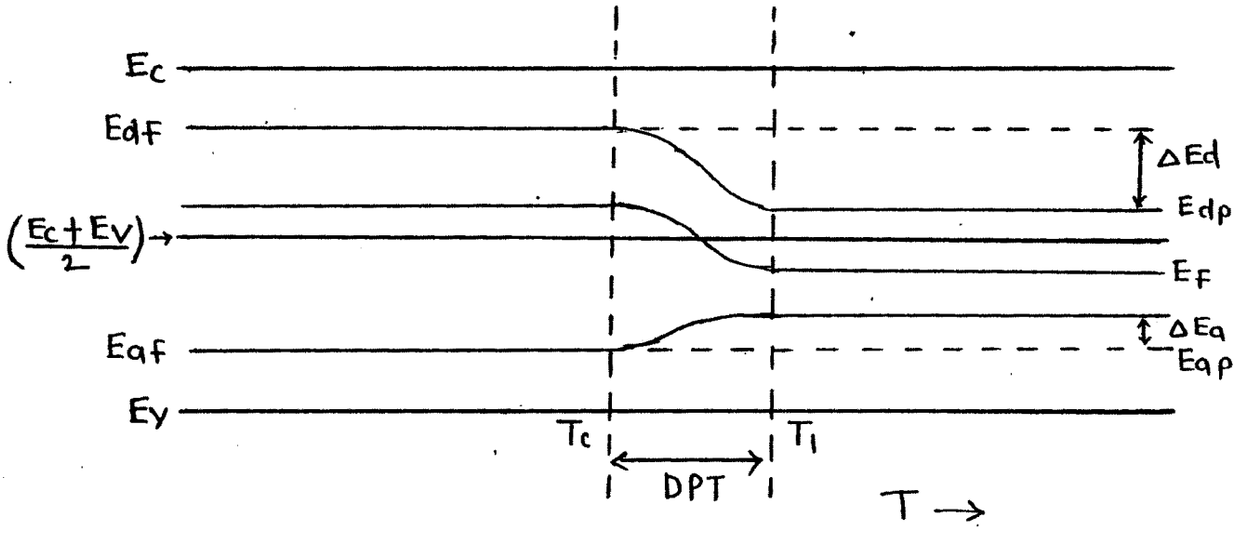

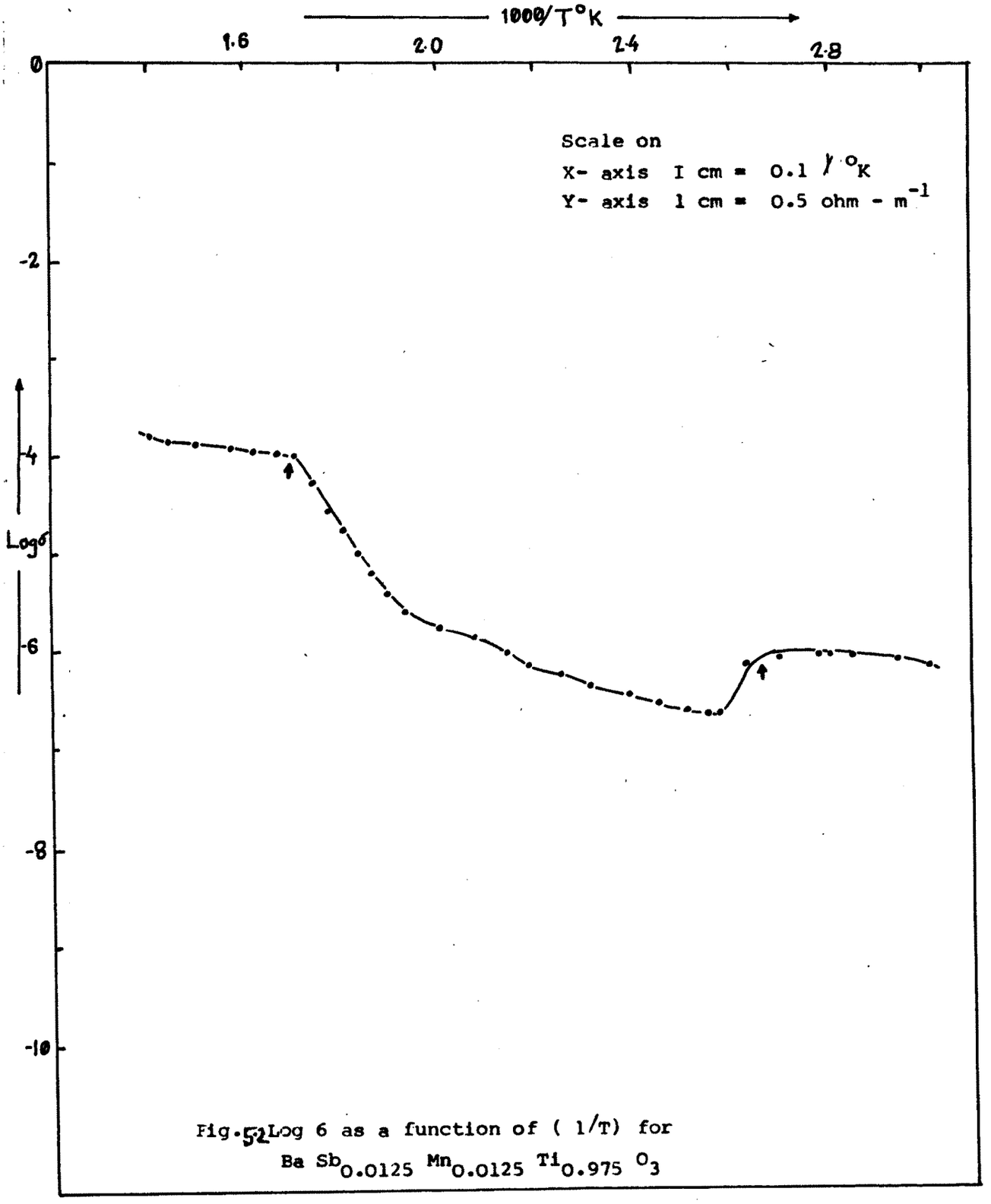

Fig. 52 Log 6 as a function of (1/T) for
Ba $Sb_{0.0125}$ $Mn_{0.0125}$ $Ti_{0.975}$ O_3

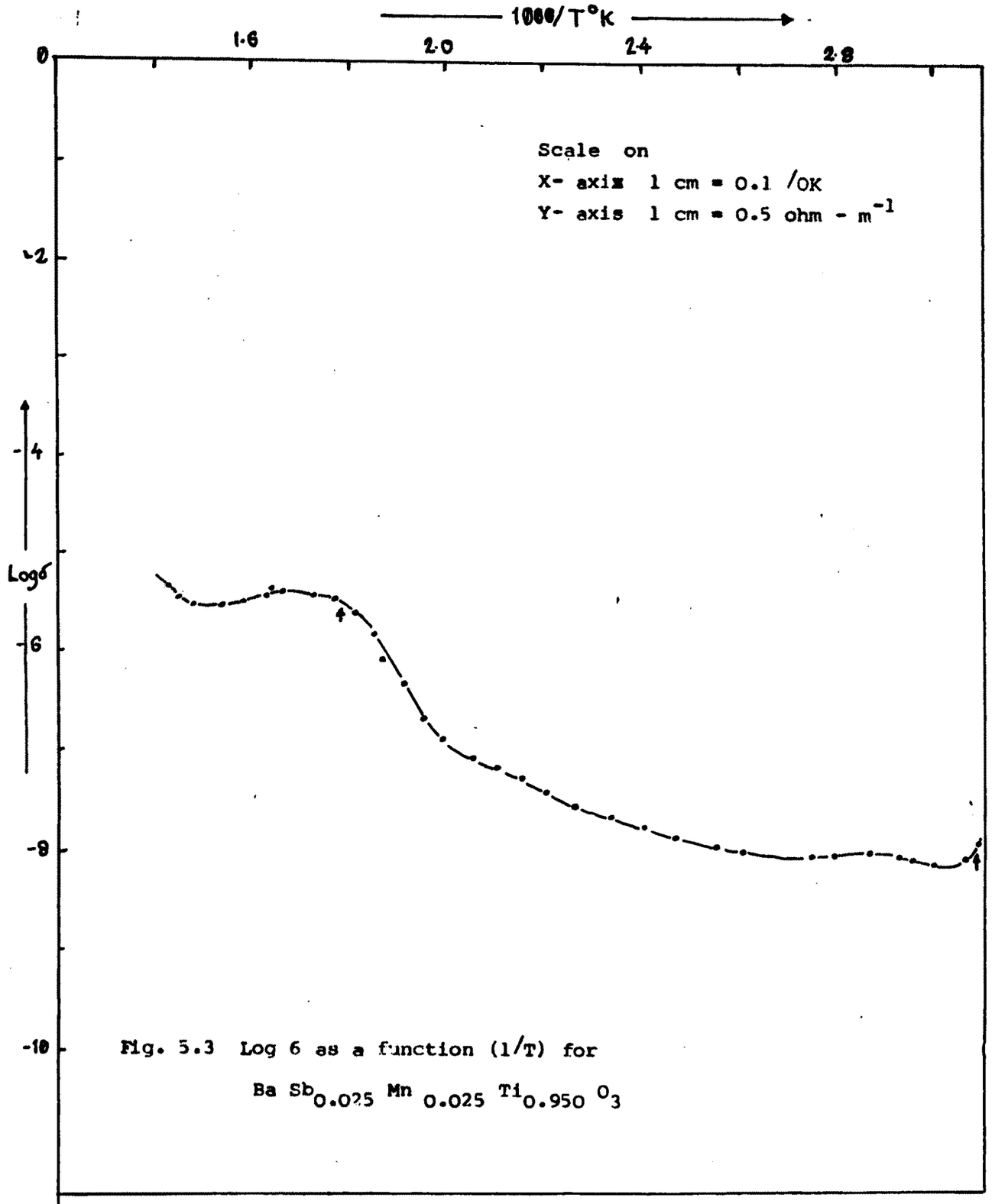

Fig. 5.3 Log 6 as a function (1/T) for

Ba $Sb_{0.025}$ Mn $_{0.025}$ $Ti_{0.950}$ O_3

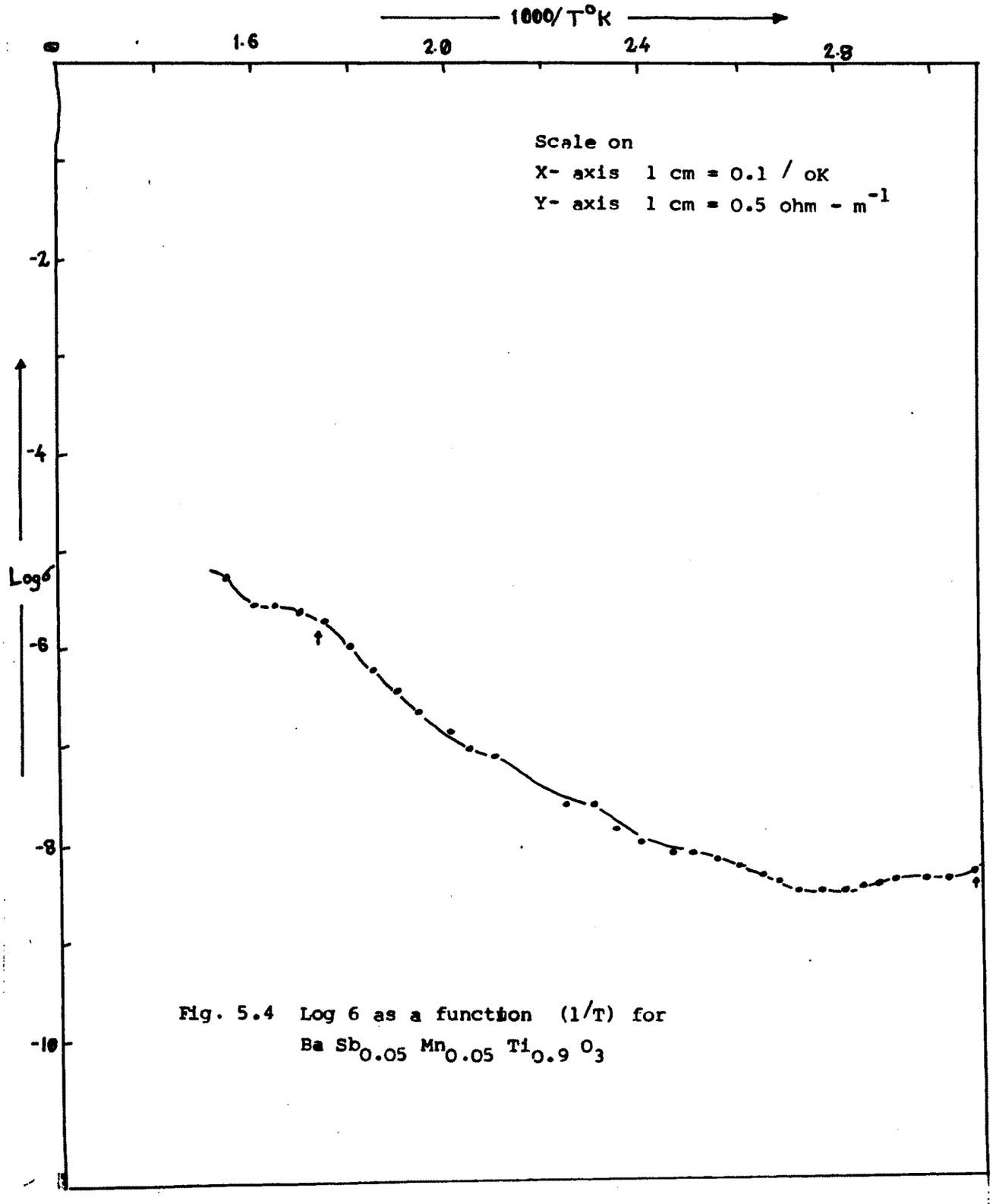

Fig. 5.4 Log 6 as a function (1/T) for
Ba $Sb_{0.05}$ $Mn_{0.05}$ $Ti_{0.9}$ O_3

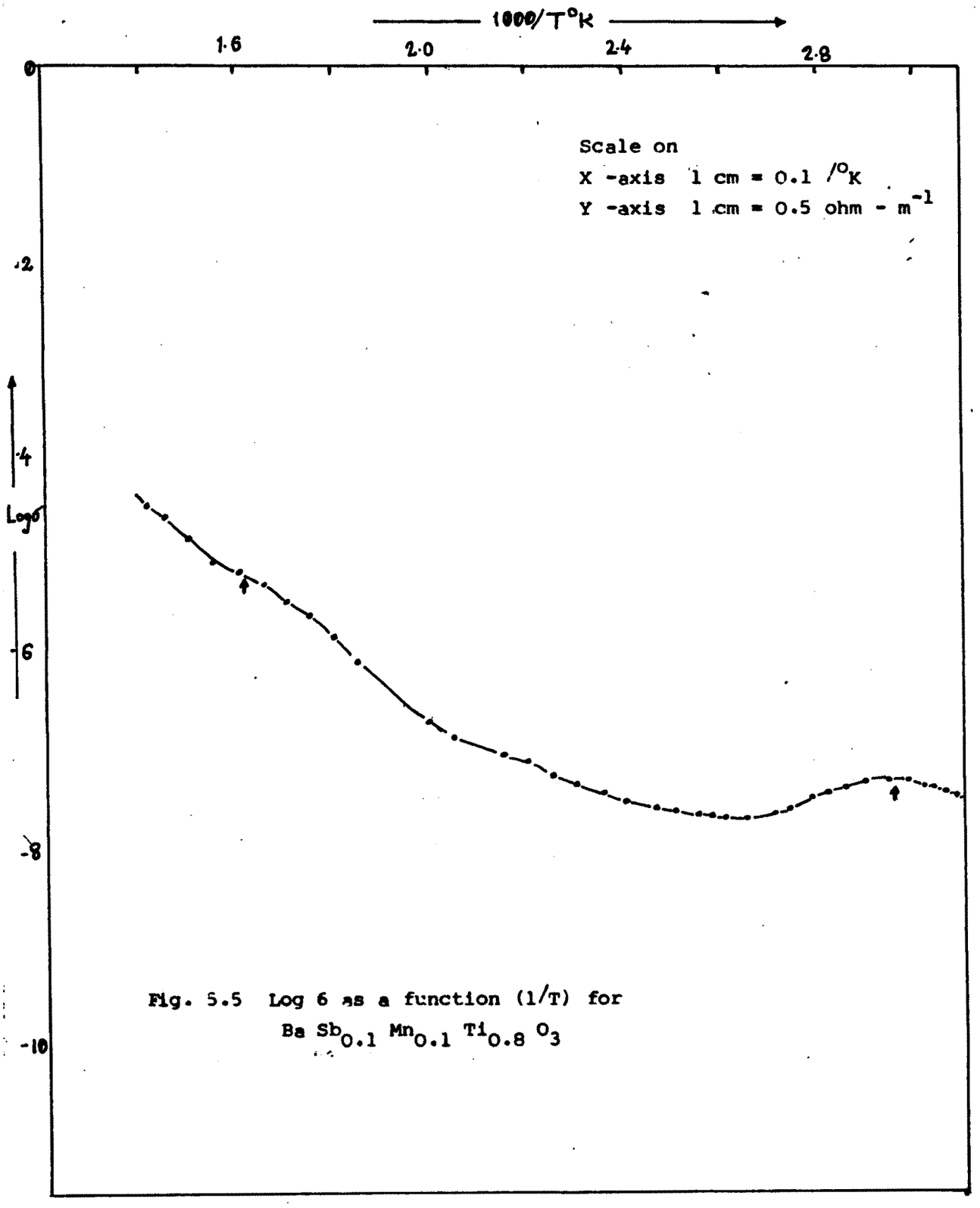

Fig. 5.5 Log 6 as a function (1/T) for
$Ba\ Sb_{0.1}\ Mn_{0.1}\ Ti_{0.8}\ O_3$

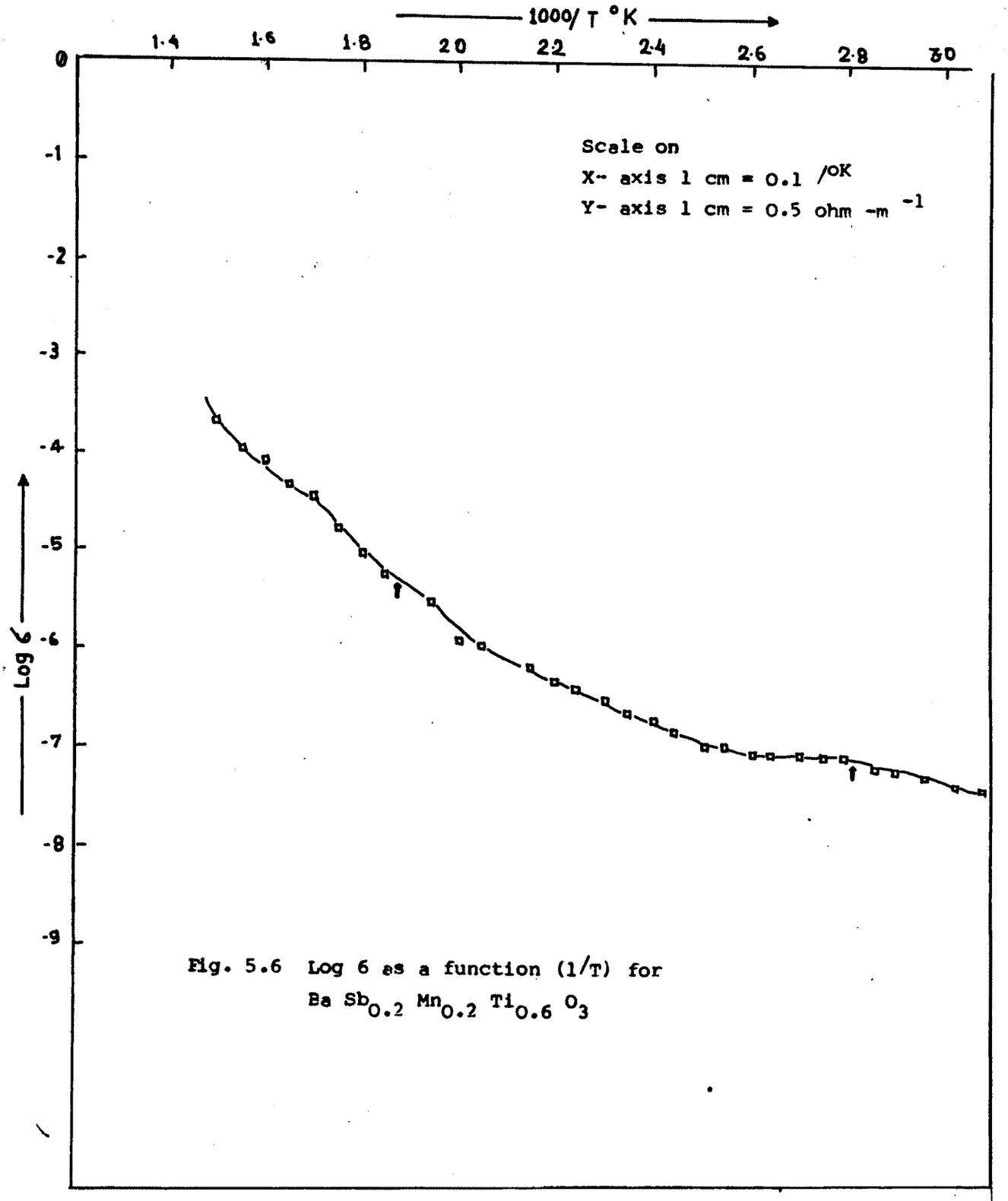

Fig. 5.6 Log 6 as a function (1/T) for
Ba $Sb_{0.2}$ $Mn_{0.2}$ $Ti_{0.6}$ O_3

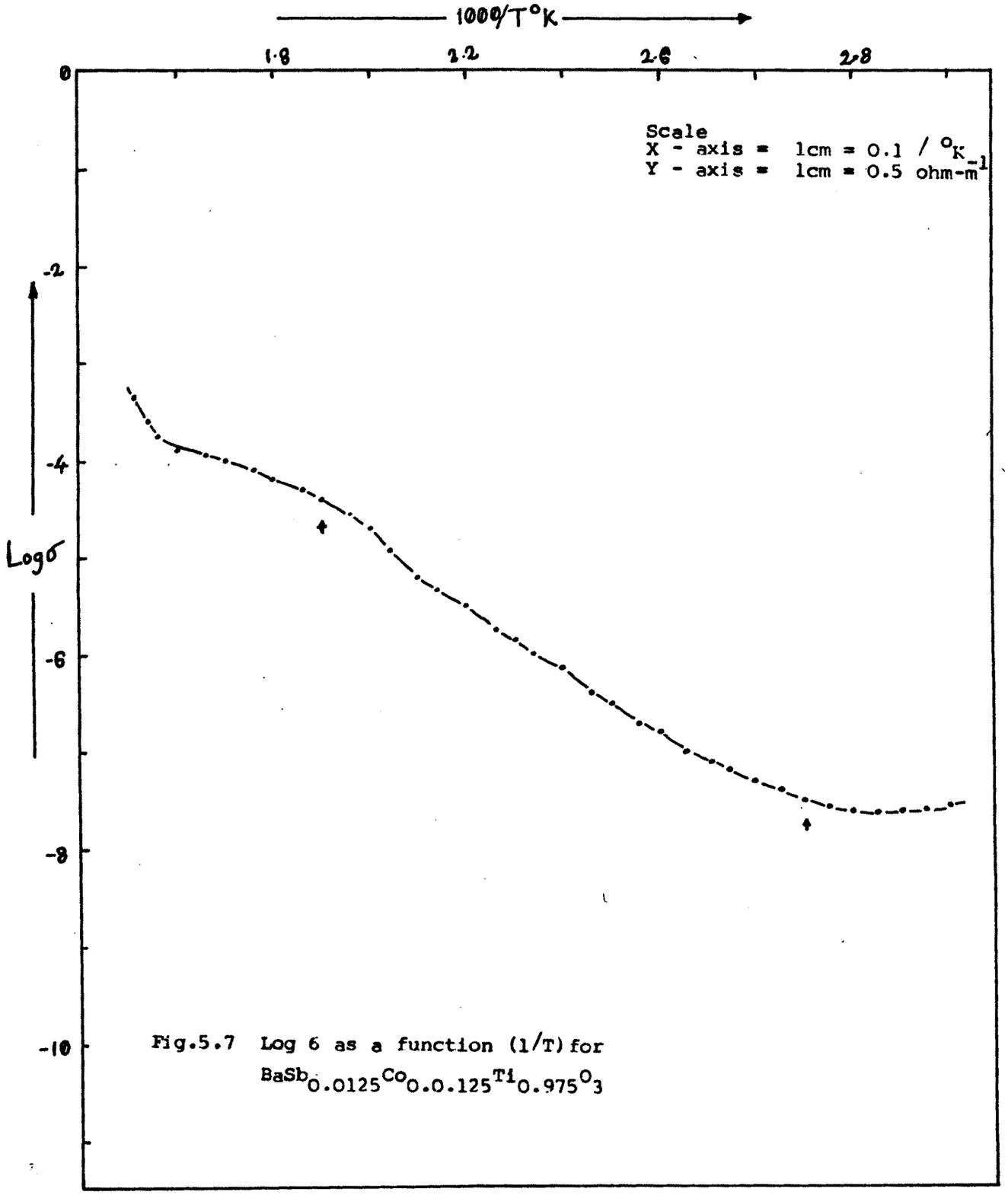

Fig.5.7 Log 6 as a function (1/T) for $BaSb_{0.0125}Co_{0.0.125}Ti_{0.975}O_3$

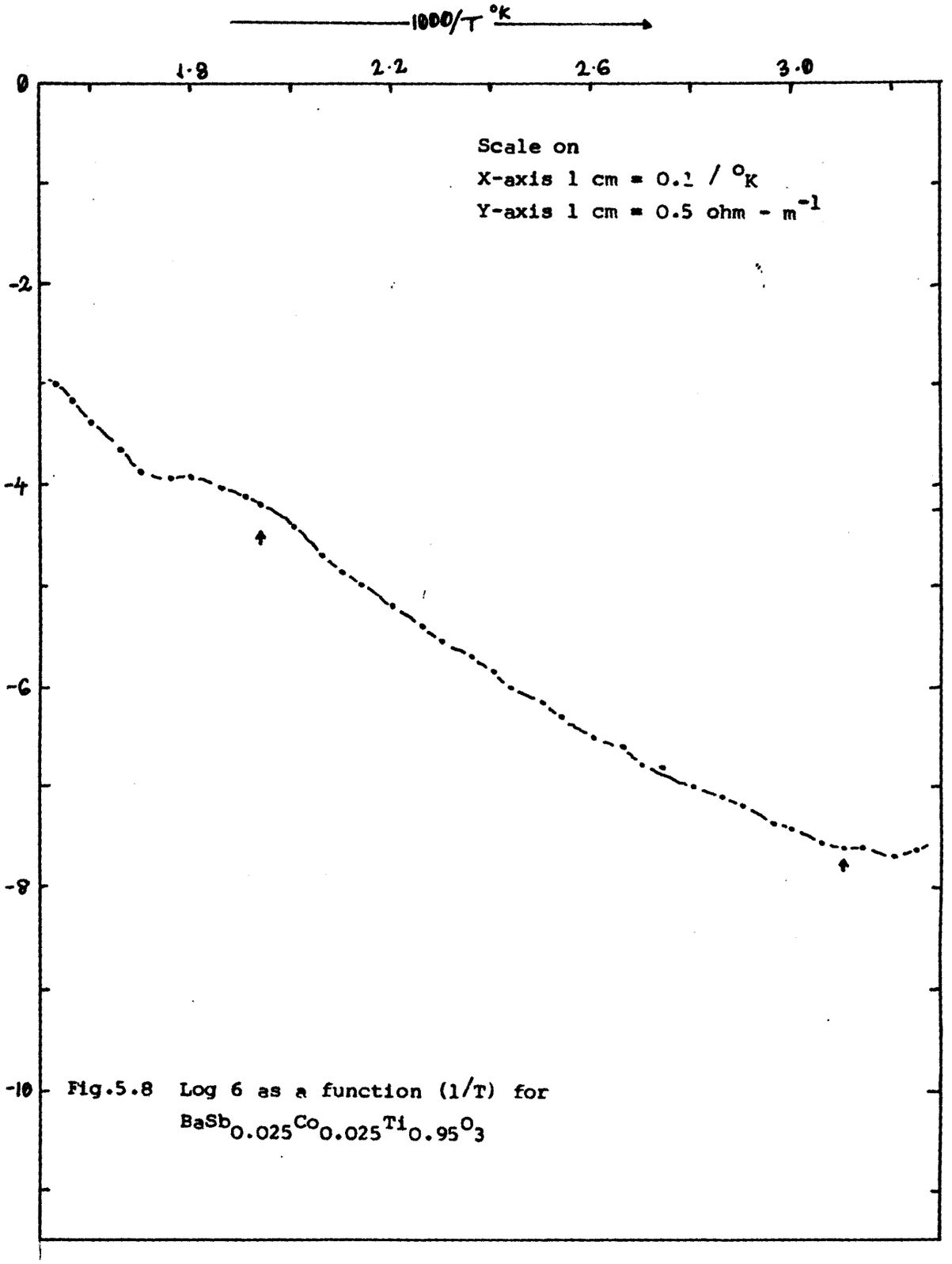

Fig.5.8 Log 6 as a function (1/T) for $BaSb_{0.025}Co_{0.025}Ti_{0.95}O_3$

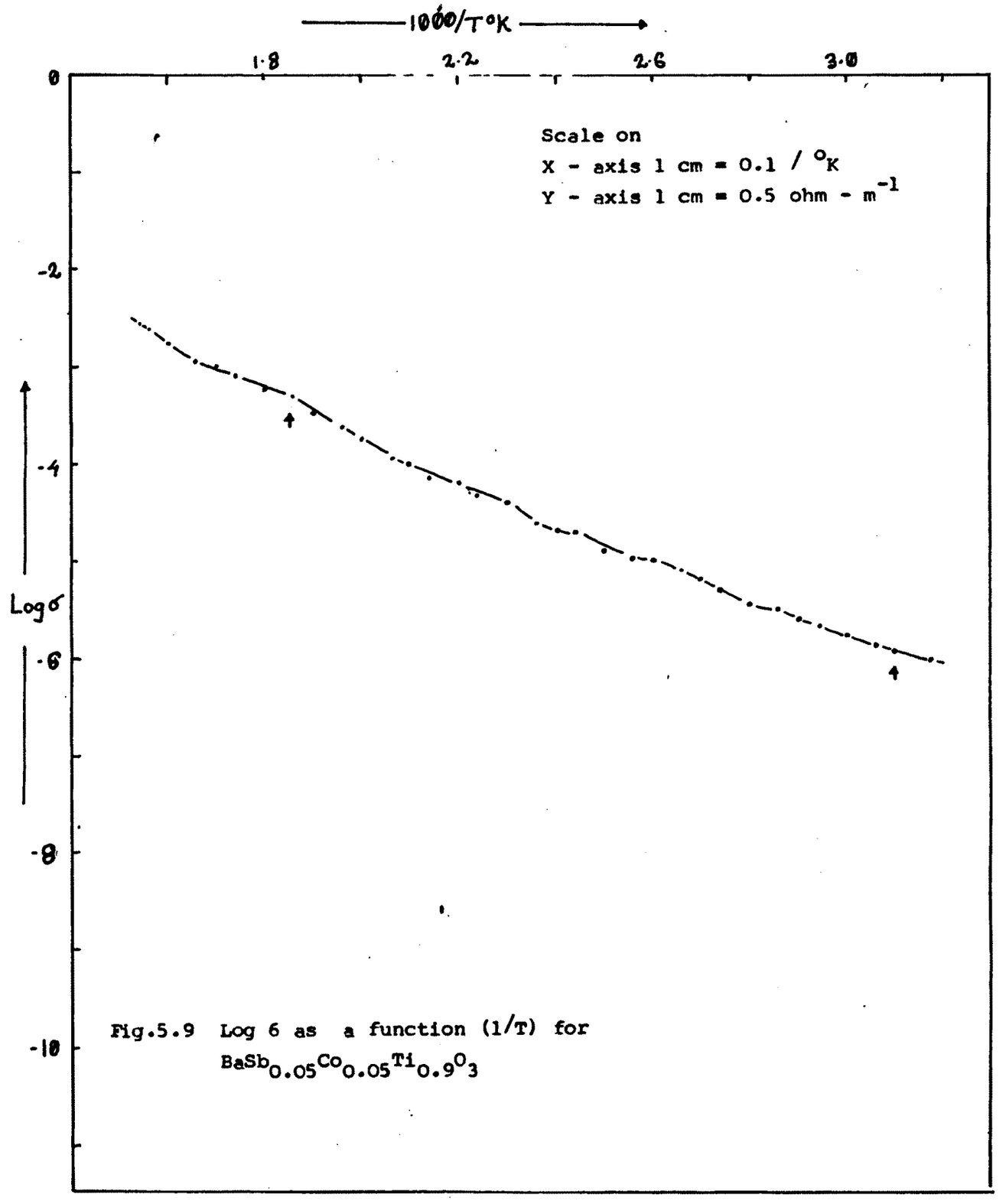

Fig.5.9 Log 6 as a function (1/T) for $BaSb_{0.05}Co_{0.05}Ti_{0.9}O_3$

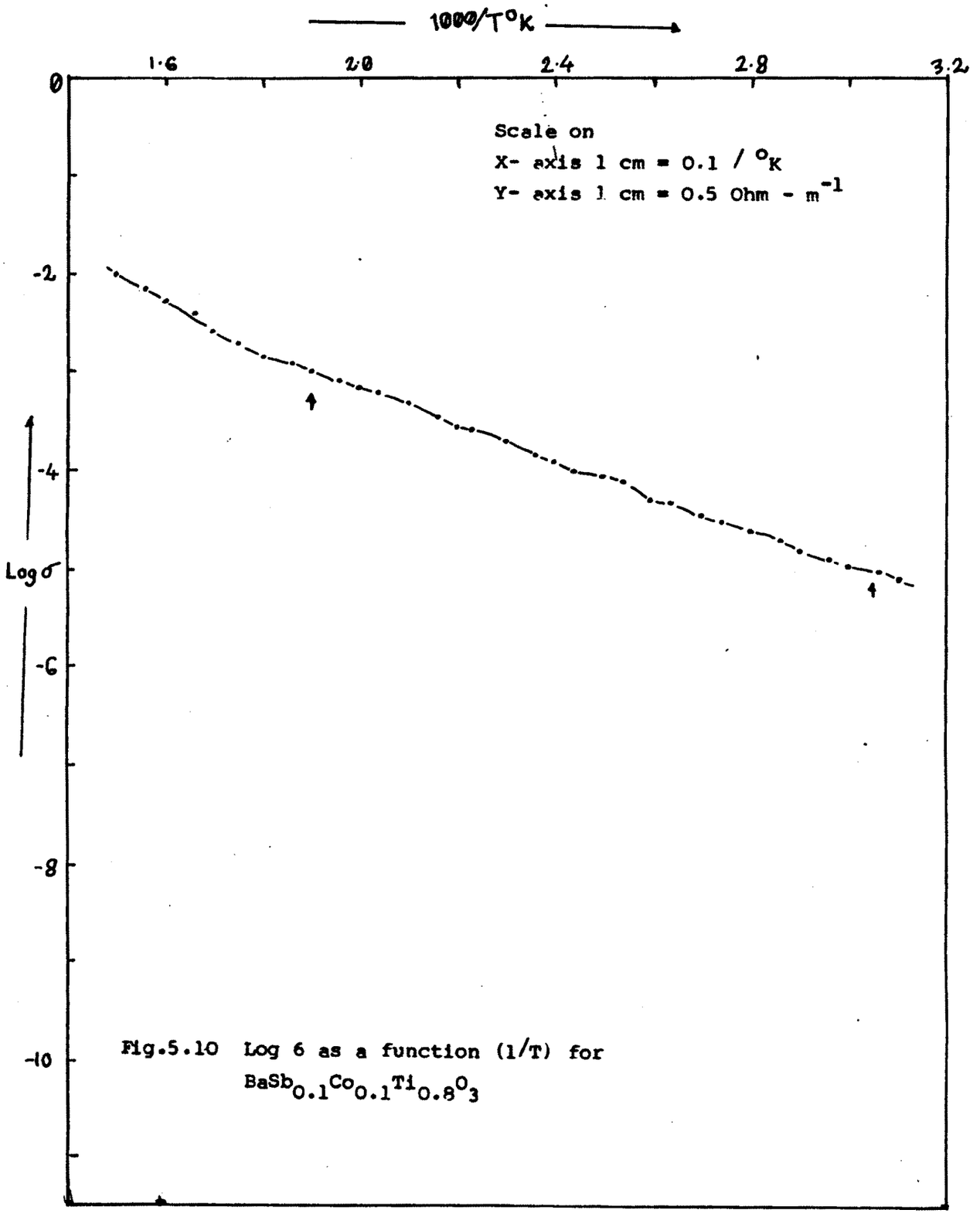

Fig.5.10 Log 6 as a function (1/T) for $BaSb_{0.1}Co_{0.1}Ti_{0.8}O_3$

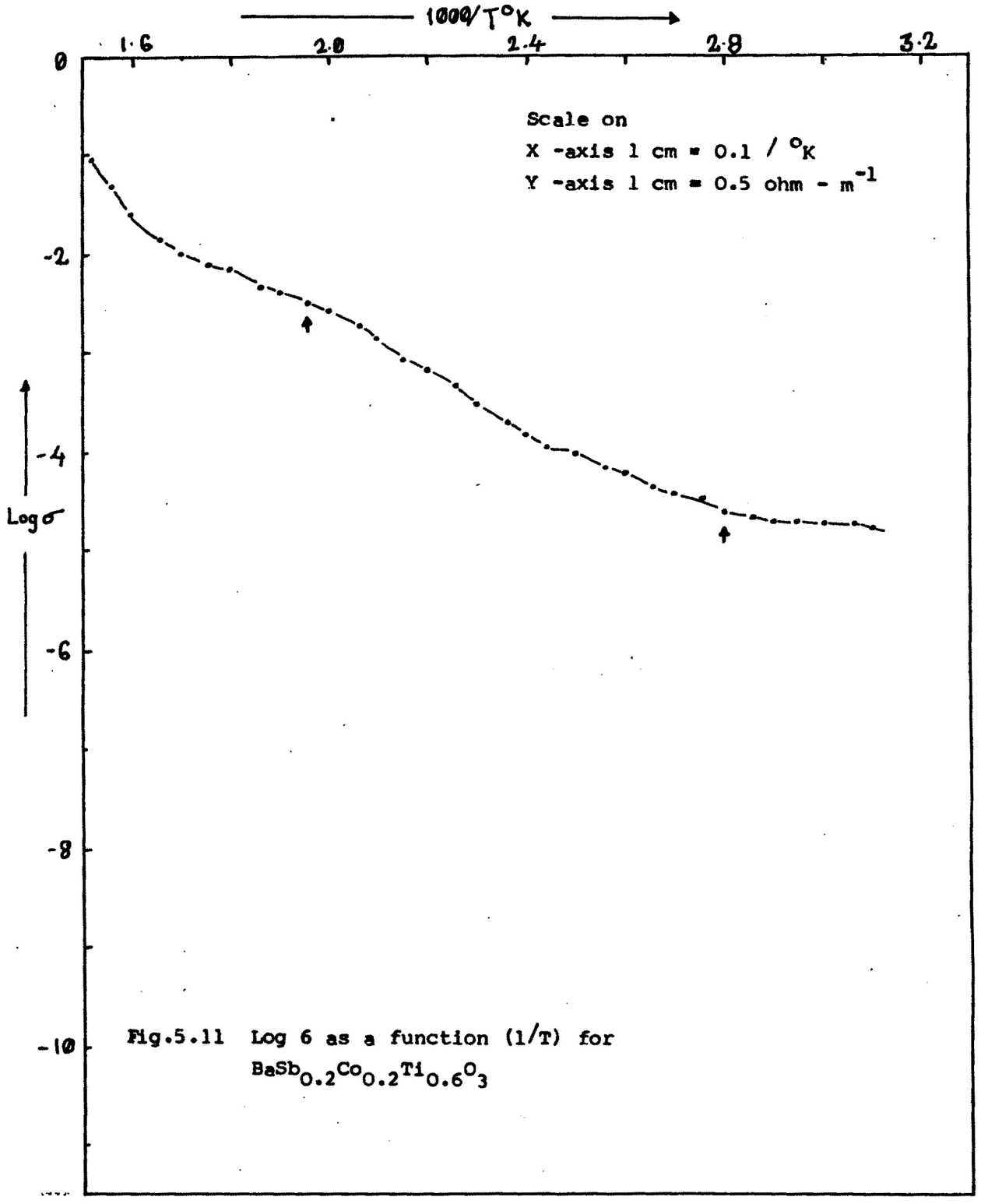

Fig.5.11 Log 6 as a function (1/T) for $BaSb_{0.2}Co_{0.2}Ti_{0.6}O_3$

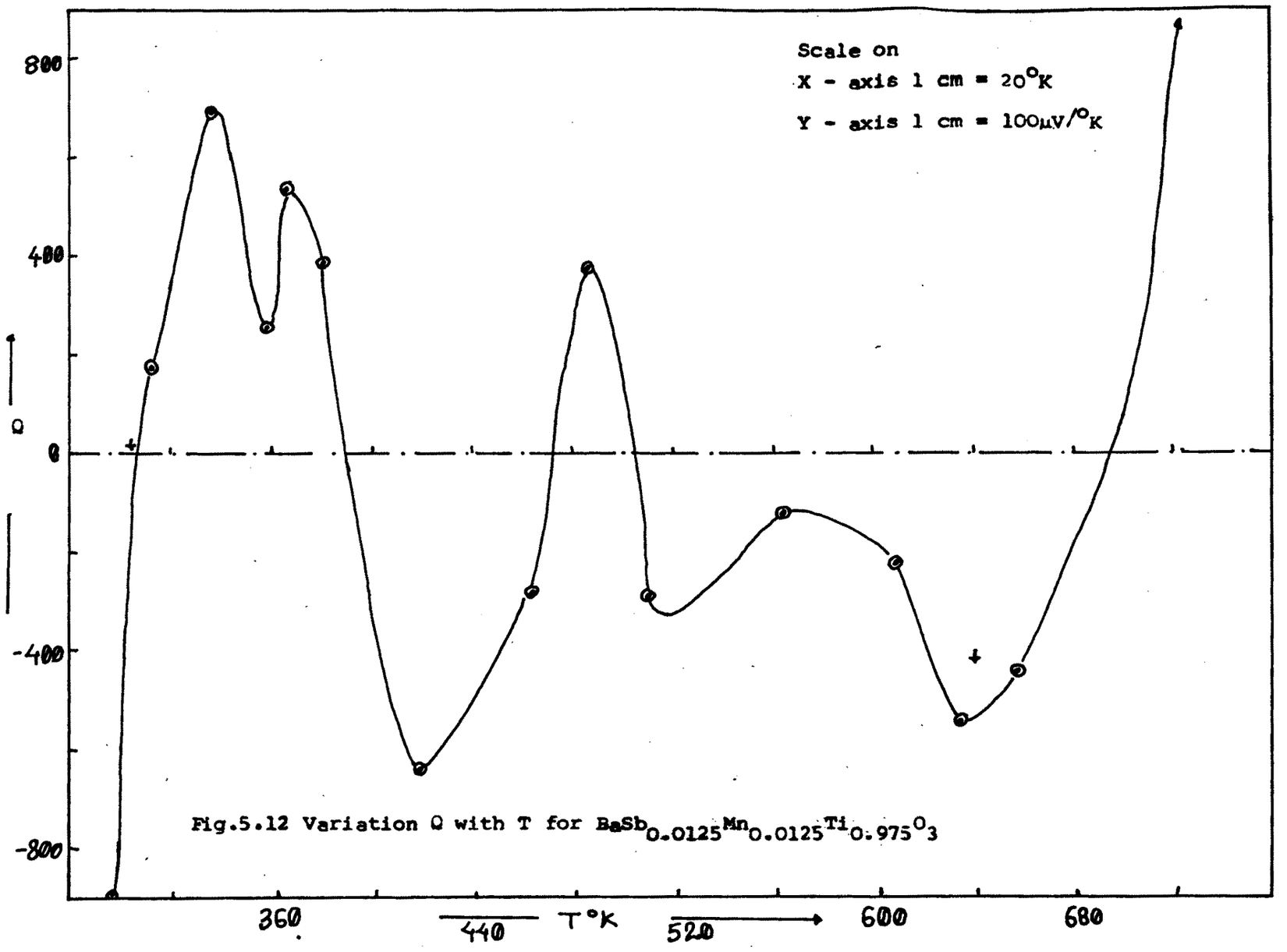

Fig.5.12 Variation Q with T for $BaSb_{0.0125}Mn_{0.0125}Ti_{0.975}O_3$

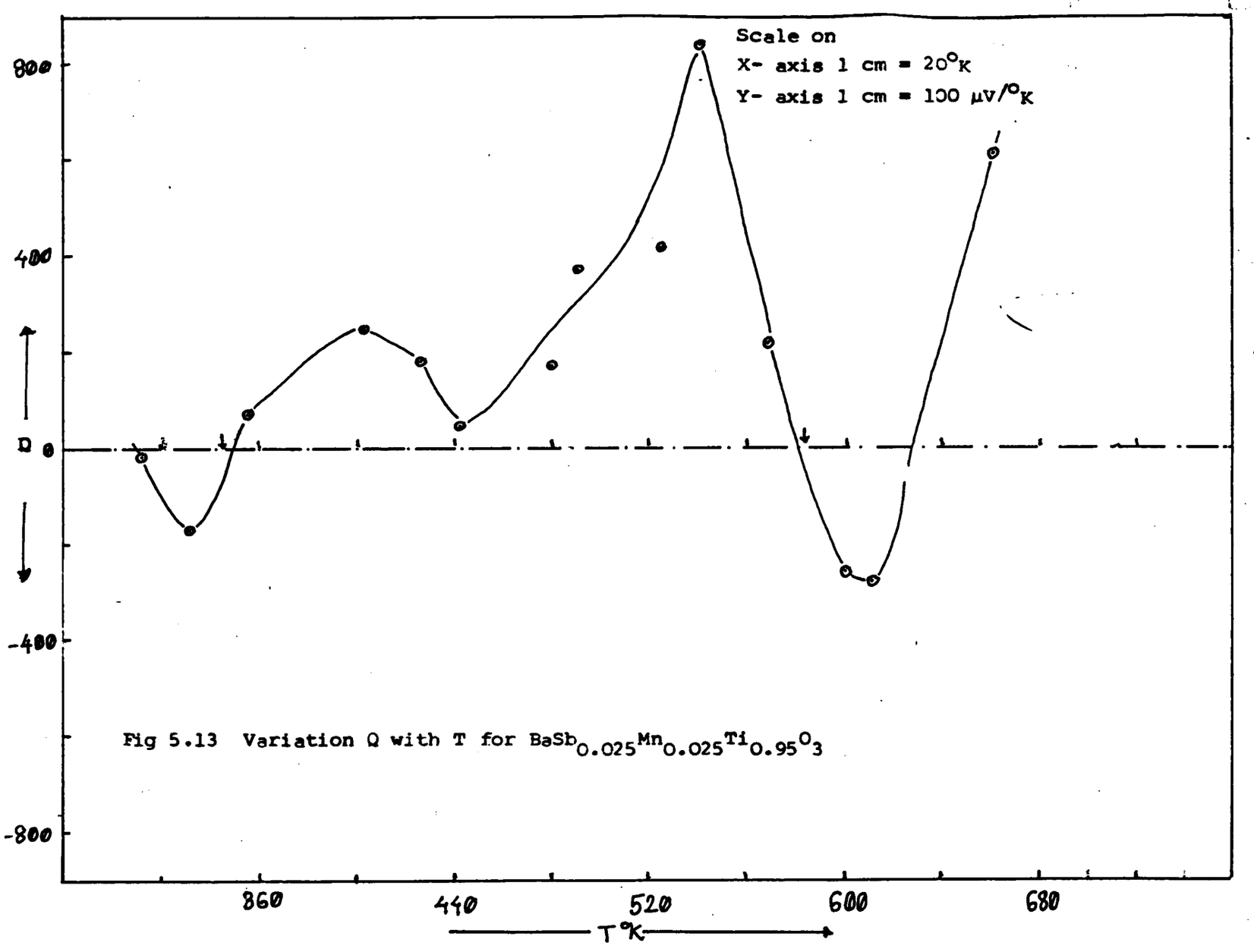

Fig 5.13 Variation Q with T for $BaSb_{0.025}Mn_{0.025}Ti_{0.95}O_3$

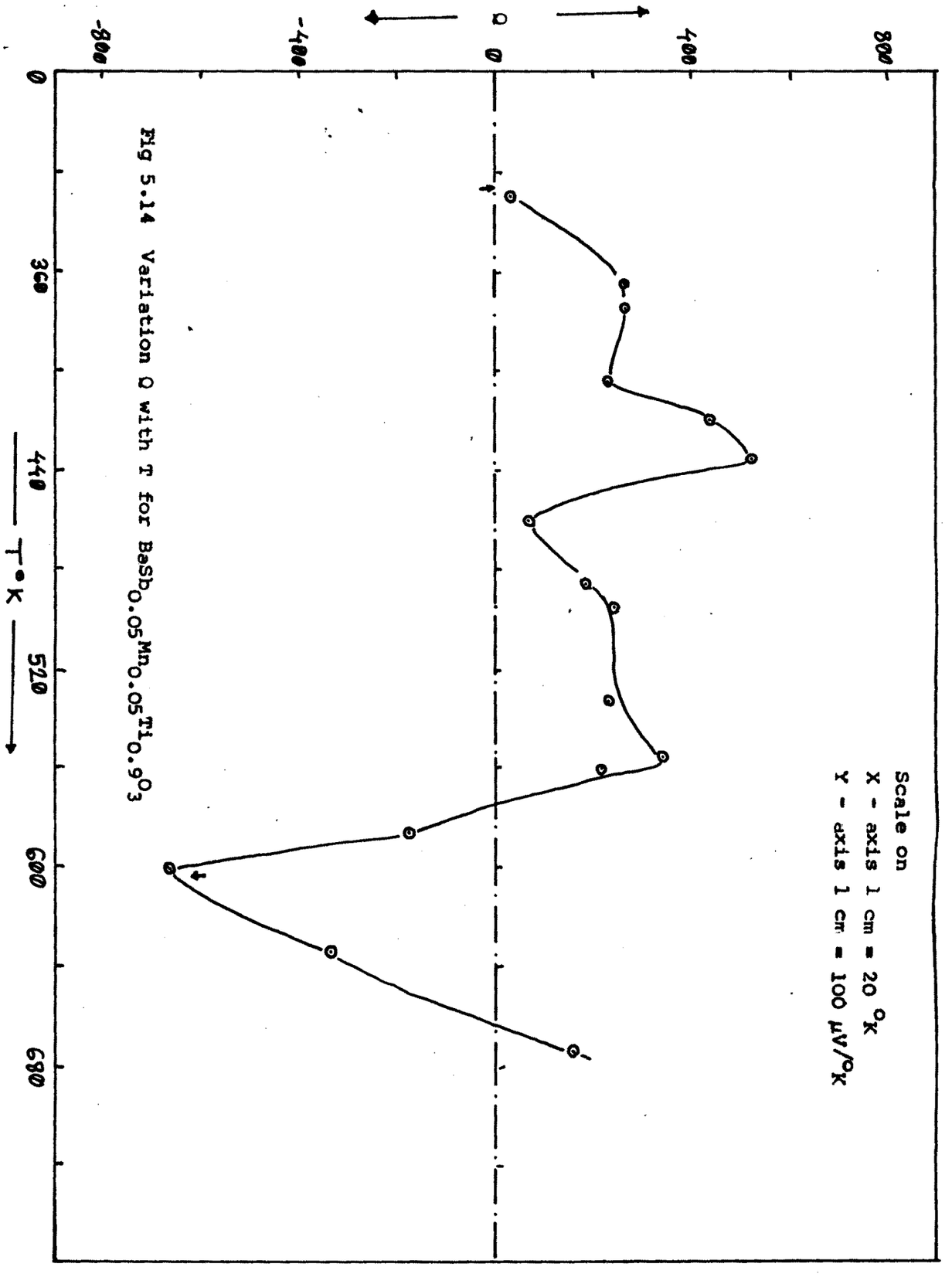

Fig 5.14 Variation Q with T for $BaSb_{0.05}Mn_{0.05}Ti_{0.9}O_3$

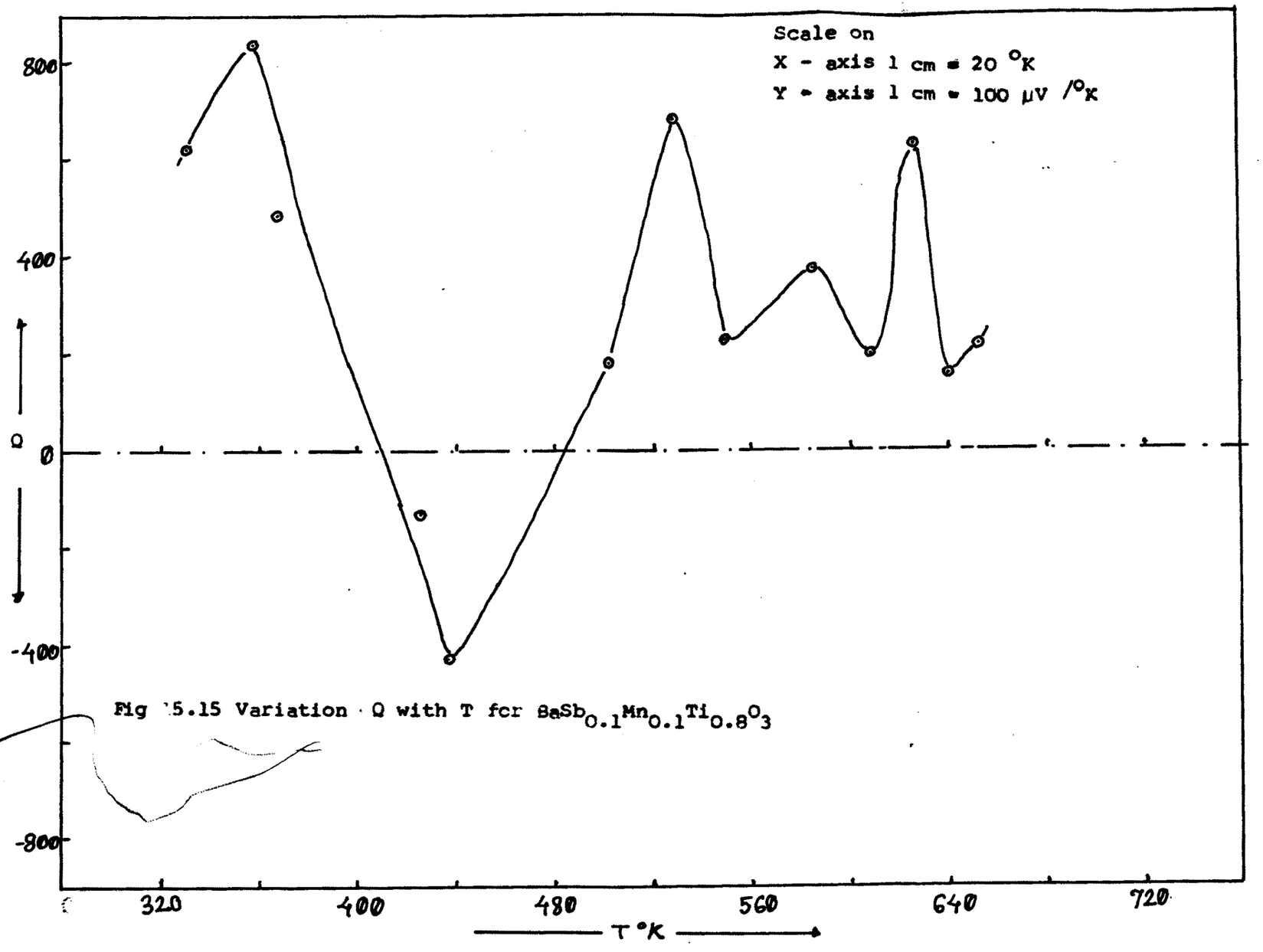

Fig 5.15 Variation of Q with T for $BaSb_{0.1}Mn_{0.1}Ti_{0.8}O_3$

resistivity shows only a break in slope , the seebeck coefficient may show a transition or a structure. We expect the structures observed in case of DPT system than the sharp transition as seen for $BaTiO_3$ single crystal.

The seebeck coefficient may provide us the information about the majority carriers or the prevailing mode of conduction, be due to the holes or due to the electrons It is observed that very pure single crystals of BaTiO 3 possess the conduction due to holes (96). For imperfect crystals or ceramics the conduction is n type below Tc, While it becomes P-type above the transition temperature. We have decided to invoke this tool to understand electron transport properties of compensating of-valency substituted perovskite in a systamatic way. At present this is just a begining and as discussed in Section 5.2.2 a model development is in progress. Before we have a model to correlate the behavior of Q as a function of T . We shall present the data , determined with improved accuracy, Section 2.2.4. At present we shall make only a few qualitative remarks about the observations.

The Fig 5.12 to 5.21 show the Q versus T behavior for Ba $Ti_{(1-x)}$ $Sb_{x/2}Mn_{x/2}$ O_3 system with x = 0.025, 0.05, 0.1, 0.2, 0.4. respectively. Ba $Ti_{(1-x)}$ $Sb_{x/2}Co_{x/2}$ O_3 system with x = 0.025, 0.05, 0.1, 0.2, 0.4. respectively.

A few general observations are as below.

1) The seebeck Coefficient shows multiple structures in the temperature range of investigations. The occurrence of these structures indicate that role of vacancies or off-valency elements have a temperature dependent predominance. As it has been discussed in the previous section we shall be interested in

the structures in the vicinity of room temperature and in the temperature range of apparent second transition.

2) All the curves show a sudden change of conduction from electronic type to hole type in the vicinity of room temperature. The change is not a transition but the 'Q' changes from negative to positive within a interval of a few degrees .The temperatures at which this change occurs are given in table 5.2.

If we compare the tables 5.1 and 5.2, it is apparent that the temperature of change over of polarity of conduction and break in slope are in the proximity of 20°C. This appears to be a quite good agreement. It is to be noted that the break in slope of ln 6 is determined only on the basis of observation and no numerical method is employed to determine exact point of break in slope.

3) The slow changeover of Q from n-type to p-type confirms the DPT behavior. Further it demands that the electron transport properties and the permittivity are to be analyzed in a correlative fashion. At present we also don't know how exactly these phenomenon would be correlated.

4) Another interesting feature is observed at temperatures in the vicinity of 550°K. In this region the Q again becomes negative for a temperature interval of nearly 20 to 40°K. These temperatures are also recorded in table 5.2. The reason for this structure could be the presence of $BaTi_3O_7$ phase (Section 2.1.2).

5) Just after transition the Q becomes positive. The values of

positive Q after transition Q is given in table 5.2 . For SbMn system the Q is 700$\mu v/^{o}K$ for x=0.025. For the increasing concentrations of SbMn the positive values of Q becomes very low ~200$\mu v/oK$ (The concentration x=0.2 is an exception,and we wish to confirm this observation by preparing fresh samples of concentration x=0.2) for SbCo system the values of positive Q increases slowly for increasing value of x. It reducess a little at x=0.4. This increase in hole type of conduction could be attributed to the increasing number of Co^{+2} ions in the SbCo compositions.

6) For SbCo compositions the magnitude of Q is comparably low.

From the discussions above we feel that the model of electronic conduction is required which can simultaneously account for the 6 and ϵr, such a model can explained the complex impedance behavior in greater depth.

Table no 5.1: Transition Temperatures for TEP Begaviour

x	Positive Thermopower after transition	T1	T2
	SbMn System		
0.025	+700	328	633
0.05	+220	345	597
0.1	+260	328	611
0.2	+840	312	557
0.4	+260	388	---
	SbCo System		
0.025	+120	303	550
0.05	+120	303	506
0.1	+130	303	542
0.2	+280	303	515
0.4	+170	375	440

Table 5.2: Temperatures of break in slope and Conductivity log 6 at room temperature.

x	T1	T2	Log 6 at R.T. -
		SbMn System	
0.025	375	593	8.6
0.05	324	561	8.0
0.1	322	581	8.2
0.2	337	584	7.5
0.4	358	537	7.6
		SbCo system	
0.025	344	526	7.58
0.05	322	515	7.62
0.1	322	540	6.17
0.2	327	526	5.18
0.4	357	512	4.88

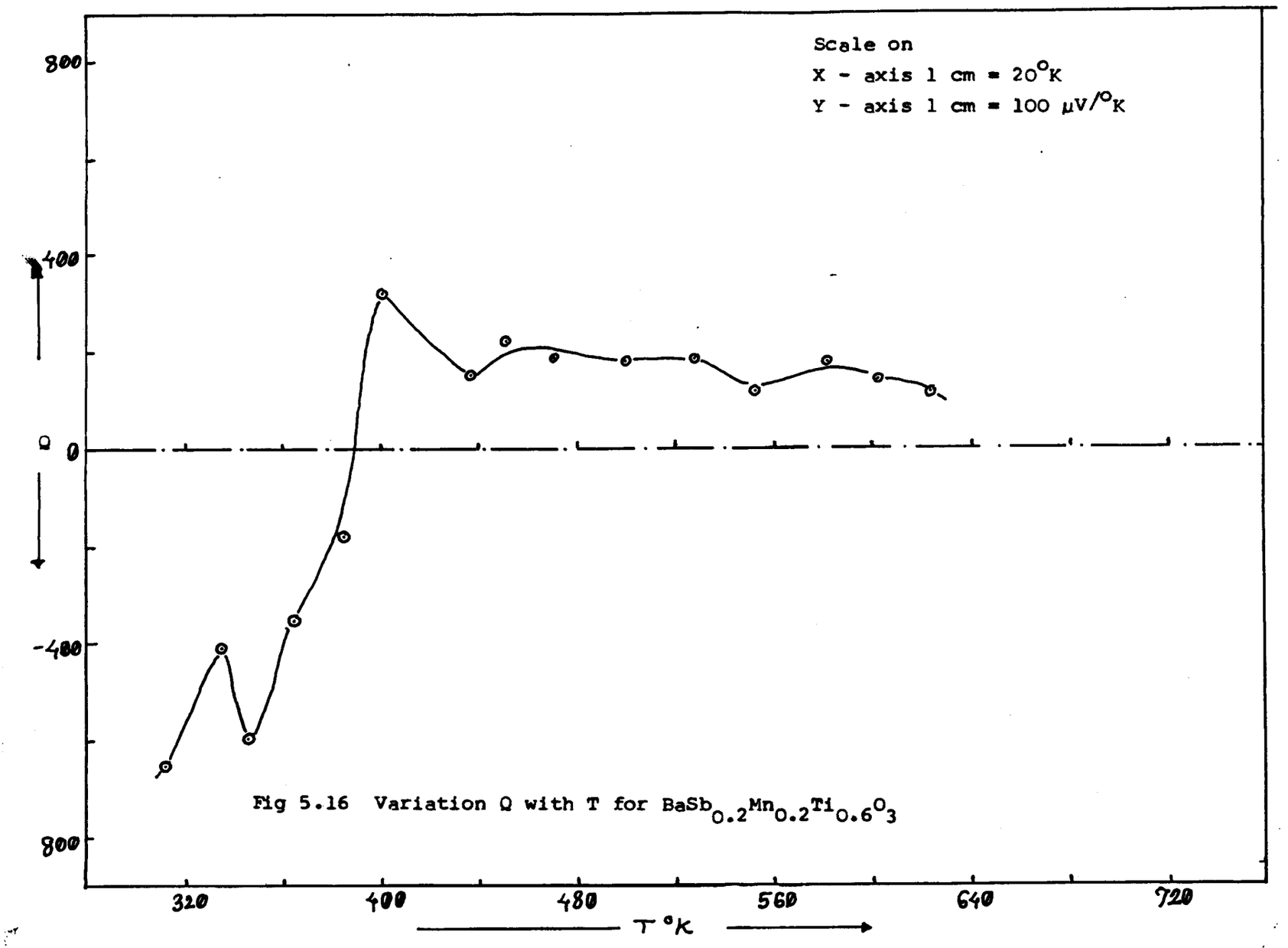

Fig 5.16 Variation Q with T for $BaSb_{0.2}Mn_{0.2}Ti_{0.6}O_3$

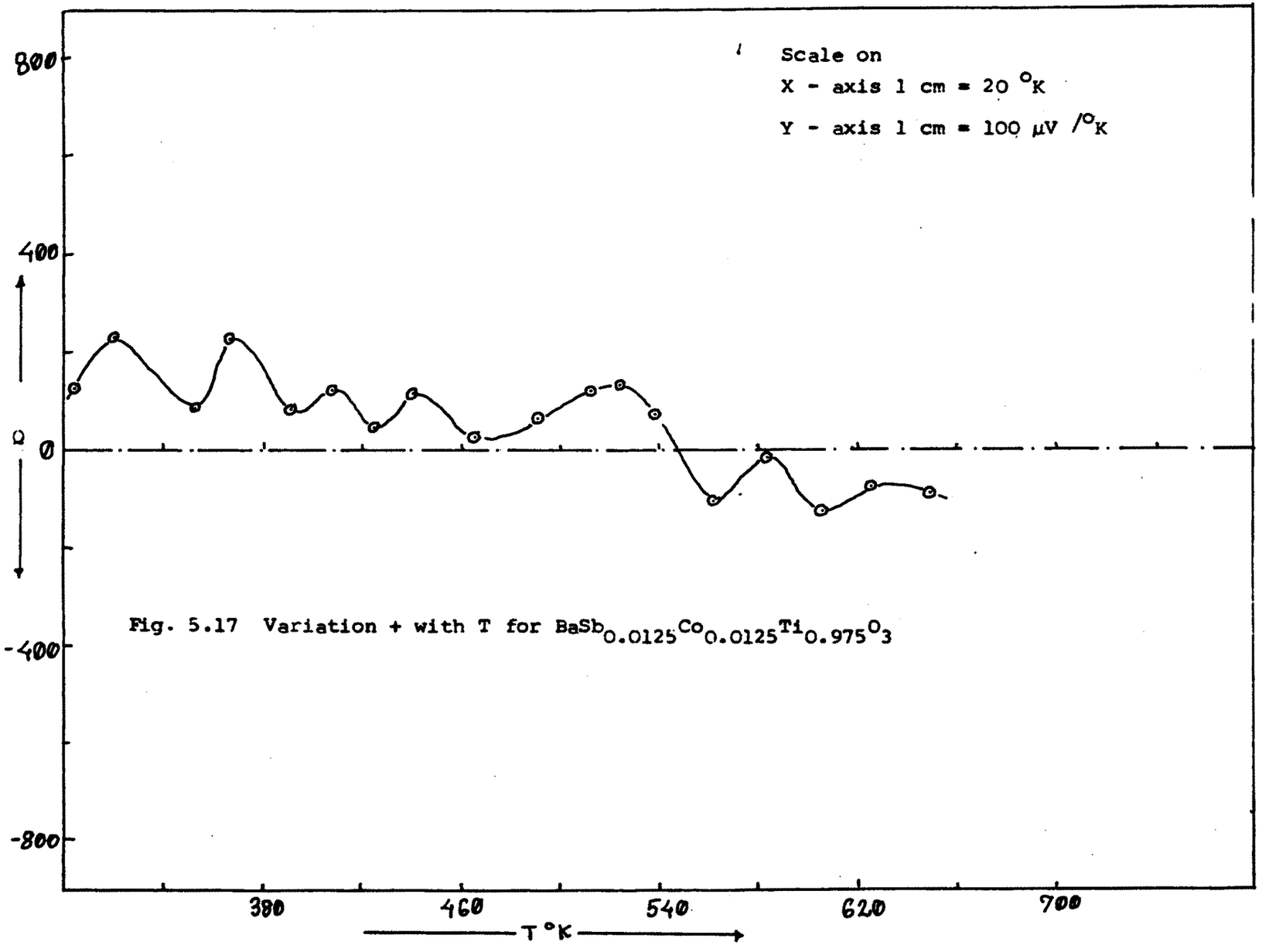

Fig. 5.17 Variation + with T for $BaSb_{0.0125}Co_{0.0125}Ti_{0.975}O_3$

Fig 5.18 Variation Q with T for $BaSb_{0.025}Co_{0.025}Ti_{0.95}O_3$

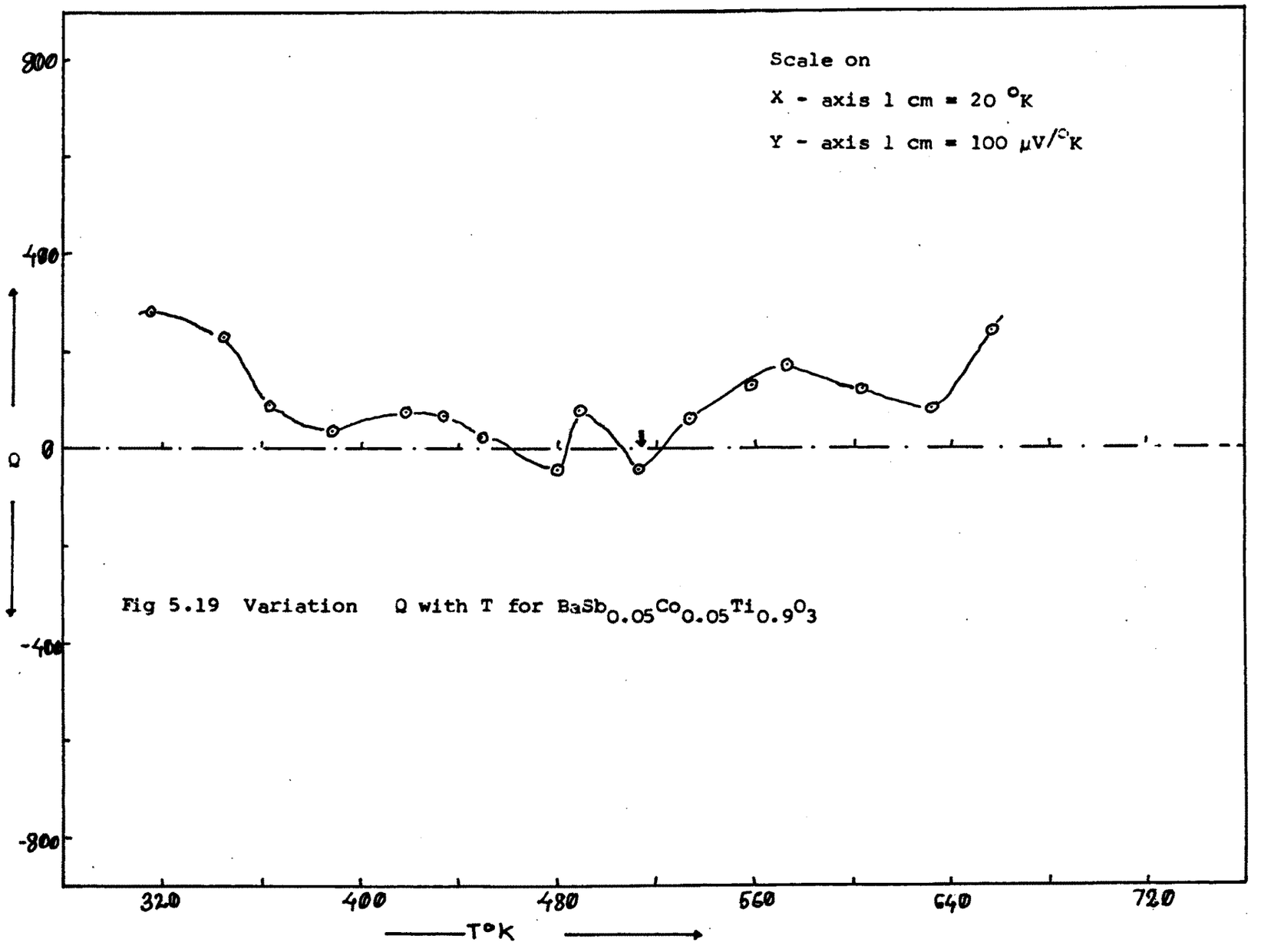

Fig 5.19 Variation Q with T for $BaSb_{0.05}Co_{0.05}Ti_{0.9}O_3$

Fig 5.20 Variation Ω with T for $BaSb_{0.1}Co_{0.1}Ti_{0.8}O_3$

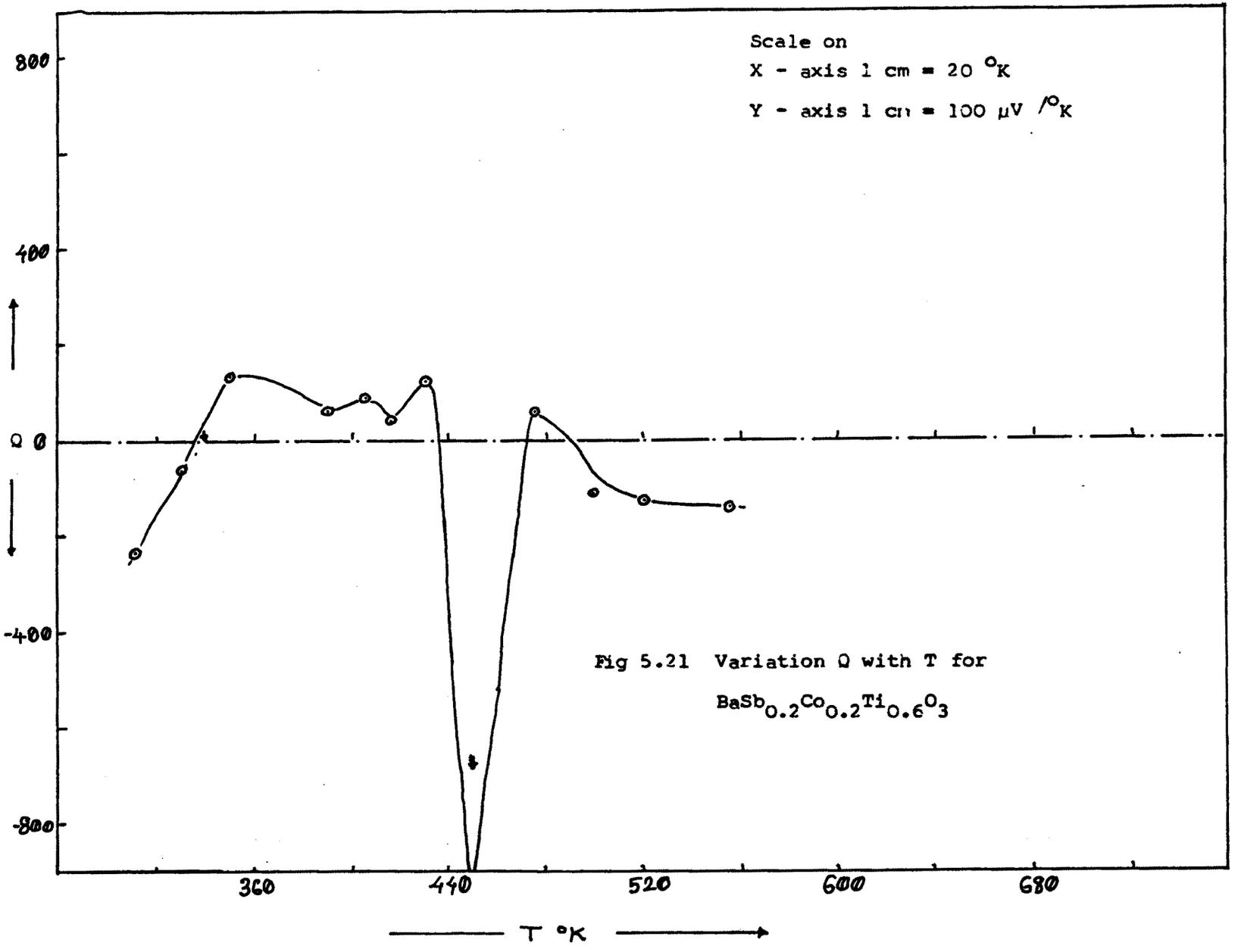

Fig 5.21 Variation Q with T for $BaSb_{0.2}Co_{0.2}Ti_{0.6}O_3$

RESUME

The present dissertation reports the syntheses, permittivity, and electron transport properties as a function of temperature of the SbMn and SbCo substituted Ba TiO_3. It has been emphasized in chapter I that more systematic investigations on the compensating off-valency substituted perovskite is required to arrive at atleast an empirical understanding of the modifications brought in by the substitutions. We feel that the understanding of the modifications in the Ti site are important as far as the phenomenon of ferroelectricity is concerned. The $BaTiO_3$ being a well studied ferroelectric material, with spherically symmetric outer shell of Ba ions, is selected as the matrix for substitution.

It is not just sufficient to select the substitutent elements but one has to design a qualitative procedure of systhesis of the mixed valency compounds. The procedure should take care of stabilizing the valancies of the various ions in the desired oxidation states we have reported such a procedure for the SbMn and SbCo substitutions. The resulting ceramics are subjected to the Structural investigations and a systmatic variation in the lattice parameter 'a' is recorded for the varying the level of substitutions. The parameter 'a'passes through a minimum for x=0.025, for SbMn system and x= 0.05 for SbCo system. The ratio c/a is independent of the level of substitution. This behavior is suggestive of the importance of intermolecular interactions in deciding the structure of the material.

The permittivity measurements on these samples are reported

as a function of temperature cyclation. A typical hysteresis is observed in the behavior of ϵ_r. The ϵ_r behaviour shows that the materials are ferroelectrics with diffused phase transition. A numerical fitting has been used to parameterize the diffusivity of the transition.

The dissertation also reports a elaborated experimental set up for the measurement of electrical conductivity and thermoemf. The thermoemf is measured using the technique of differential measurement. The over all behavior of δ is non Arrhenius. The thermoelectric power measurements confirmed the DPT and above transition, the hole type carriers predominate the conduction mechanism. We could record a consistency and systematics in the interparameter and intraparameter behavior of T.

To investigate the phenomenon of off-valency substitution further, a need of the measurements of the complex impedance and correlation of all the properties within the frame work of a single model is emphasized in the conclusion of the dissertation.